

ALGEBRAIC HYBRIDIZATION AND STATIC CONDENSATION WITH APPLICATION TO SCALABLE $H(\text{div})$ PRECONDITIONING *

V. DOBREV[†], T. KOLEV[†], C. S. LEE[†], V. TOMOV[†], AND P. S. VASSILEVSKI[†]

Abstract. We propose an unified algebraic approach for static condensation and hybridization, two popular techniques in finite element discretizations. The algebraic approach is supported by the construction of scalable solvers for problems involving $H(\text{div})$ -spaces discretized by conforming (Raviart-Thomas) elements of arbitrary order. We illustrate through numerical experiments the relative performance of the two (in some sense dual) techniques in comparison with a state-of-the-art parallel solver, ADS [24], available in [1] and [2]. The superior performance of the hybridization technique is clearly demonstrated with increased benefit for higher order elements.

Key words. static condensation, hybridization, algebraic multigrid, mixed finite elements, ADS, $H(\text{div})$ solvers, radiation-diffusion transport.

AMS subject classifications. 65F10, 65N20, 65N30

1. Introduction. This paper proposes a unified algebraic approach of constructing reduced problems by two popular techniques in the finite element method: static condensation and hybridization. It also discusses approaches for constructing scalable preconditioners for these reduced problems. The present work is motivated by the solution of problems arising in variety of finite element simulations and of particular interest is the case when the problems involve the function space $H(\text{div})$ (L_2 -vector functions that have their weak divergence in L_2). Such problems naturally arise in the mixed finite element method for Darcy equation [6], Brinkman equation [27], as well as in the FOSLS (first order system least-squares) discretization approach, [11]. Also, certain formulations of radiation-diffusion transport [9], lead to problems involving the space $H(\text{div})$. This is in fact one of the practical examples from a more realistic simulation that we consider in our numerical tests.

Highly scalable solvers for $H(\text{div})$ problems have been designed in the past. The most successful ones, of ADS-type [24], were based on the *regular decomposition* theory developed by Hiptmair and Xu [20]. Although of optimal complexity, the current state-of-the-art ADS algorithms are quite involved and require also going through solvers for $H(\text{curl})$, such as AMS, [23]. Both solvers, ADS and AMS, require some additional user input (e.g., discrete gradient), which makes them not completely *algebraic*. The results of the present paper can be viewed as a further step towards the design of fully algebraic solvers for problems involving $H(\text{div})$.

To design faster, yet still scalable, alternative to ADS, we employ a traditional finite element technique commonly used in mixed finite elements referred to as *hybridization*. This is perhaps the first technique proposed to solve the saddle-point problems arising in the mixed methods, since it leads to symmetric and positive definite (SPD) reduced problems. Its early form appeared in a paper by Fraeijis de Veubeke in 1965 [17] as an efficient solution strategy for elasticity problems. In [3], Arnold and Brezzi studied the method from a theoretical perspective, and obtained

* This work was performed under the auspices of the U.S. Department of Energy by Lawrence Livermore National Laboratory under Contract DE-AC52-07NA27344, and sponsored by the U.S. Department of Energy, Office of Science, Office of Advanced Scientific Computing Research, Applied Mathematics program. LLNL-JRNL-732140.

[†]Center for Applied Scientific Computing, Lawrence Livermore National Laboratory, P.O. Box 808, L-561, Livermore, CA 94551, U.S.A (dobrev1@llnl.gov, tzanio@llnl.gov, cslee@llnl.gov, tomov2@llnl.gov, panayot@llnl.gov).

error estimates for all the unknowns involved; see also [8]. The technique was further developed by Cockburn and Gopalakrishnan to allow approximations by polynomials of different degree in different subregions; see for example [14] and [15] for applications to mixed finite element approximations of second order scalar elliptic problems and Stokes flow.

Another very popular technique in finite elements is *static condensation*. It is a reduction technique intended to reduce the size of a linear system of finite element equations by eliminating at element or subdomain level internal degrees of freedom (dofs). It was also first introduced in the structural analysis literature in 1965, cf., [18, 21, 28], and has been widely used since then. Static condensation neglects the dynamic effect in the reduction, hence the name. On element level, one can eliminate locally degrees of freedom that are not shared by neighboring elements (a typical case for high order elements). Thus, the reduced, Schur complement, problem contains only shared (interface) dofs. If the elimination is performed on a subdomain level, the resulting reduced system coincides with the one in the balancing domain decomposition by constraints (BDDC) algorithm [16]. Recently, BDDC preconditioners with deluxe scaling and adaptive selection of primal constraints for $H(\text{div})$ problems have been developed, see for instance [26, 29, 30]. The approach in the present paper, on the other hand, solves the reduced system by algebraic multigrid (AMG).

For $H(\text{div})$ -conforming elements (i.e., elements that have only shared dofs through common faces), both static condensation and hybridization lead to reduced problems of the same size (equal to the number of shared interface dofs). If one applies these two approaches not on element level, but for subdomains (union of elements), substantial reduction in size can be achieved. Thus, these two approaches are of great practical interest and the goal of the present paper is to study them in a common framework, emphasize their similarities and differences, and most importantly, design new, or modify existing solution techniques that are efficient and scalable, achieving substantial savings compared to the state-of-the-art solvers for the original problems. For problems obtained by static condensation, there has been success in modifying the state-of-the-art solvers (AMS and ADS) to be directly applicable to the reduced problem, cf., [10, 5]. In this paper, we focus on the design of scalable solvers for problems involving $H(\text{div})$ in a general algebraic setting, extending the preliminary results in [25].

The remainder of the paper is organized as follows. In Section 2, we describe the algebraic hybridization approach and show how it can serve as an alternative to traditional finite element assembly. Next, we deduce its relation to static condensation and the mixed hybridized finite element method in Section 3. Preconditioning strategies for the reduced systems obtained from hybridization and static condensation are discussed in Section 4. Then we describe the implementation details of the methods and present some numerical examples in Section 5 and Section 6 respectively. Finally, we conclude the paper in Section 7.

2. Two perspectives of finite element assembly. In this section we describe the traditional process of finite element assembly, and introduce algebraic hybridization as an alternative process to obtain a global linear system describing the same finite element discretization.

2.1. Finite element assembly components. To fix notation, consider a bilinear form $a(\cdot, \cdot)$ and a linear form $f(\cdot)$ over a Hilbert space \mathcal{H} defining the Galerkin

weak variational formulation: Find $u \in \mathcal{H}$, such that for all $v \in \mathcal{H}$, we have

$$a(u, v) = f(v).$$

In the finite element method, we introduce a triangulation $\mathcal{T} = \mathcal{T}_h$ of the given computational domain and decompose the forms into sums of their local element versions, i.e. $a(\cdot, \cdot) = \sum_{\tau \in \mathcal{T}} a_\tau(\cdot, \cdot)$ and $f(\cdot) = \sum_{\tau \in \mathcal{T}} f_\tau(\cdot)$. We further replace \mathcal{H} with a finite dimension space induced by \mathcal{T}_h and on each element $\tau \in \mathcal{T}$ we compute a local *element stiffness matrix* A_τ and a *load vector* \mathbf{f}_τ by using the element basis functions in the local bilinear and linear forms. We are assuming that A_τ (which correspond to $a_\tau(\cdot, \cdot)$) are SPD. The latter holds for example if the bilinear form $a(u, v)$ contains a mass term, $\int \beta uv \, dx$, with a positive coefficient $\beta = \beta(x) > 0$.

2.2. The traditional finite element assembly procedure. A central concept in the finite element method is that of *assembly* – the accumulation of local stiffness matrices A_τ and load vectors \mathbf{f}_τ into a global matrix A and a global vector \mathbf{f} which form the (global) linear system

$$A\mathbf{x} = \mathbf{f}, \tag{2.1}$$

for the unknown vector of finite element degrees of freedom. The $n \times n$ matrix A is SPD and generally sparse, i.e., the number of its nonzero entries, $\text{nnz}(A)$, is $\mathcal{O}(n)$.

Let $\hat{A} = \text{blockdiag}(A_\tau)$ be the $\hat{n} \times \hat{n}$ block-diagonal matrix with all element stiffness matrices on its main diagonal, and $\hat{\mathbf{f}}$ be similarly the $\hat{n} \times 1$ vector containing all element load vectors. The finite element method produces a global-to-local mapping, P , which maps global dofs into local ones for each element. That is, for a $n \times \hat{n}$ matrix P , the traditional assembly process can be written as the triple matrix product that relates A and \hat{A} , and a matrix-vector product that builds the global right-hand side,

$$A = P^T \hat{A} P, \quad \text{and} \quad \mathbf{f} = P^T \hat{\mathbf{f}}. \tag{2.2}$$

In the simplest case the action $\hat{\mathbf{x}} = P\mathbf{x}$ simply means copying the values of the global dof vector \mathbf{x} to the corresponding local values, independently in each element. More complicated P can account for non-conforming mesh refinement as we describe in some detail in a following section. Either way, (2.2) is a formalized expression for the traditional process of finite element assembly.

2.3. Algebraic hybridization. It is classical in the finite element literature to introduce (2.1) as the global linear system that corresponds to the finite element discretization specified by \hat{A} , $\hat{\mathbf{f}}$ and P . As we describe next, there is an alternative global linear system corresponding to the same solution, which in certain cases is advantageous from the perspective of linear solvers. To introduce this alternative, let C be another matrix such that

$$\text{Null}(C) = \text{Range}(P),$$

i.e. a vector z satisfies $Cz = 0$, if and only if there is a vector y , such that $z = Py$. In particular, we have the matrix equality $CP = 0$.

We assume that P is full column rank and that C is full row rank. Similarly to P , the matrix C could also be provided algebraically by the finite element space, e.g. the columns of C^T can be constructed by orthogonally completing the basis given by

the columns of P . (The matrix C is not unique and there are other ways to construct it as illustrated later in the paper.)

The idea of algebraic hybridization is that instead of adding the different element contributions of $\hat{A}, \hat{\mathbf{f}}$, we use C to enforce equality constraints of the decoupled vector $\hat{\mathbf{x}}$ through a new Lagrange multiplier variable $\boldsymbol{\lambda}$. This process is known as *hybridization* in the context of mixed finite element method [7], but in this section we consider it on a purely algebraic level, independent of the particular continuous problem or finite element discretization approach. In fact, the C -based reformulation can be described in more general terms than classical assembly, which we do in the following main linear algebra result.

THEOREM 2.1. *Let \hat{A} , P and C be matrices of size $\hat{n} \times \hat{n}$, $\hat{n} \times n$ and $m \times \hat{n}$ ($m = \hat{n} - n$) respectively, such that \hat{A} is SPD, P is full column rank, C is full row rank, and $\text{Null}(C) = \text{Range}(P)$. Also, let $\hat{\mathbf{f}}$ be a column vector of size \hat{n} . Then the problem*

$$P^T \hat{A} P \mathbf{x} = P^T \hat{\mathbf{f}}, \quad (2.3)$$

is equivalent to the following, hybridized, saddle-point system

$$\begin{bmatrix} \hat{A} & C^T \\ C & 0 \end{bmatrix} \begin{bmatrix} \hat{\mathbf{x}} \\ \boldsymbol{\lambda} \end{bmatrix} = \begin{bmatrix} \hat{\mathbf{f}} \\ 0 \end{bmatrix}. \quad (2.4)$$

Specifically, the saddle-point system (2.4) is uniquely solvable and the solution $\hat{\mathbf{x}}$ of (2.4) and \mathbf{x} (the solution of the original system), are related as

$$\hat{\mathbf{x}} = P\mathbf{x}.$$

The solution $\hat{\mathbf{x}}$ is computable via standard (block-)Gaussian elimination: we first compute the Schur complement system for the Lagrange multiplier

$$H\boldsymbol{\lambda} \equiv C\hat{A}^{-1}C^T\boldsymbol{\lambda} = C\hat{A}^{-1}\hat{\mathbf{f}}, \quad (2.5)$$

then, by back substitution, we have

$$\hat{\mathbf{x}} = \hat{A}^{-1}(\hat{\mathbf{f}} - C^T\boldsymbol{\lambda}).$$

Proof. The saddle-point system is invertible due to our assumptions; namely, \hat{A} is SPD (hence invertible), and C^T is full column rank, hence the (negative) Schur complement $H = C\hat{A}^{-1}C^T$ is also SPD and invertible. From $\hat{A}\hat{\mathbf{x}} + C^T\boldsymbol{\lambda} = \hat{\mathbf{f}}$ and $CP = 0$, we obtain

$$P^T \hat{A} \hat{\mathbf{x}} = P^T \hat{\mathbf{f}} =: \mathbf{f}.$$

Now, since $C\hat{\mathbf{x}} = 0$ (the second equation of (2.4)), and from the assumption $\text{Null}(C) = \text{Range}(P)$, it follows that there is an \mathbf{x} such that $\hat{\mathbf{x}} = P\mathbf{x}$. Then from $\mathbf{f} = P^T \hat{A} \hat{\mathbf{x}} = P^T \hat{A} P \mathbf{x}$, we see that this \mathbf{x} is unique; namely, \mathbf{x} is the unique solution of the original problem (2.3). \square

We can summarize the results of the theorem and the previous section by stating that $P^T \hat{A} P$ and $C\hat{A}^{-1}C^T$ are equally valid global matrices for the same problem. In the case of finite elements, the first one corresponds to assembly, while the second one is the hybridized system for Lagrange multipliers.

Note that the condition that P has full column rank is equivalent to the existence of a left inverse of P : there is an $n \times \hat{n}$ matrix R such that $RP = I$, e.g. $R = (P^T P)^{-1} P^T$. We can use this restriction matrix R to compute the solution \mathbf{x} of (2.3) from the solution $\hat{\mathbf{x}}$ of (2.4) as $\mathbf{x} = R\hat{\mathbf{x}}$. Furthermore, if instead of $\hat{\mathbf{f}}$ we have access only to the assembled right-hand side vector $\mathbf{f} = P^T \hat{\mathbf{f}}$, we can use $\tilde{\mathbf{f}} = R^T \mathbf{f}$ in (2.4) instead of $\hat{\mathbf{f}}$ since $P^T \tilde{\mathbf{f}} = P^T \hat{\mathbf{f}} = \mathbf{f}$.

Note also that the first set of equations in (2.4),

$$\hat{A}\hat{\mathbf{x}} = \hat{\mathbf{f}} - C^T \boldsymbol{\lambda}.$$

can be interpreted as a local version of the problem (in a weak form), where the term $C^T \boldsymbol{\lambda}$ plays the role of a dual vector for Neumann-type boundary conditions. Indeed, if we integrate by parts locally, we get

$$\hat{A}\hat{\mathbf{x}} = \hat{\mathbf{f}} - \hat{F}$$

where \hat{F} is the Neumann data for $\hat{\mathbf{x}}$ tested against the test functions in each element. Since the exact solution satisfies (2.3), we have $P^T \hat{F} = 0$, i.e. $\hat{F} = C^T \boldsymbol{\lambda}$ for some $\boldsymbol{\lambda}$ by $\text{Null}(P^T) = \text{Range}(C^T)$. One can then think of hybridization as prescribing Neumann data for local problems from one set of $\boldsymbol{\lambda}$ values and then imposing the fact that the local solutions (fluxes) should match on their shared dofs to derive equations for $\boldsymbol{\lambda}$; for more details, see [22].

The result of Theorem 2.1 can be extended to more general settings that relax the conditions that \hat{A} and P are full column rank. This is illustrated in the next theorem.

THEOREM 2.2. *Assume that \hat{A} is a square matrix (without assuming that it is SPD or even invertible) and that $\text{Null}(C) = \text{Range}(P)$ (without assuming that P has full column rank and C has full row rank). Then equations (2.3) and (2.4) are equivalent in the following sense*

- *If \mathbf{x} solves (2.3) then there exists $\boldsymbol{\lambda}$ such that $(\hat{\mathbf{x}} = P\mathbf{x}, \boldsymbol{\lambda})$ solves (2.4).*
- *If $(\hat{\mathbf{x}}, \boldsymbol{\lambda})$ solves (2.4) then there exists \mathbf{x} that solves (2.3) such that $P\mathbf{x} = \hat{\mathbf{x}}$.*

If, in addition, we assume that \hat{A} is invertible then equations (2.4) and (2.5) are also equivalent in the following sense

- *If $(\hat{\mathbf{x}}, \boldsymbol{\lambda})$ solves (2.4) then $\boldsymbol{\lambda}$ solves (2.5).*
- *If $\boldsymbol{\lambda}$ solves (2.5) then $(\hat{\mathbf{x}} = \hat{A}^{-1}(\hat{\mathbf{f}} - C^T \boldsymbol{\lambda}), \boldsymbol{\lambda})$ solves (2.4).*

Proof. Assume that \mathbf{x} solves (2.3) and set $\hat{\mathbf{x}} = P\mathbf{x}$. We need to show that there exists $\boldsymbol{\lambda}$ such that $(\hat{\mathbf{x}}, \boldsymbol{\lambda})$ solves (2.4). The second equation in (2.4) follows from $C\hat{\mathbf{x}} = CP\mathbf{x} = 0$. The defining condition for $\boldsymbol{\lambda}$ is

$$\hat{A}\hat{\mathbf{x}} + C^T \boldsymbol{\lambda} = \hat{\mathbf{f}}, \quad \text{or} \quad C^T \boldsymbol{\lambda} = \hat{\mathbf{f}} - \hat{A}\hat{\mathbf{x}} =: \hat{\mathbf{g}}.$$

By (2.3), we have that $P^T \hat{\mathbf{g}} = 0$, i.e. $\hat{\mathbf{g}} \in \text{Null}(P^T)$. Since we have

$$\text{Null}(P^T) = \text{Range}(P)^\perp \subseteq \text{Null}(C)^\perp = \text{Range}(C^T),$$

the existence of the required Lagrange multiplier $\boldsymbol{\lambda}$ is proven.

Assume now that $(\hat{\mathbf{x}}, \boldsymbol{\lambda})$ solves (2.4). On one hand, the second equation in (2.4) is $C\hat{\mathbf{x}} = 0$, i.e. $\hat{\mathbf{x}} \in \text{Null}(C)$ and since $\text{Null}(C) \subseteq \text{Range}(P)$, there exists \mathbf{x} such that $P\mathbf{x} = \hat{\mathbf{x}}$. On the other hand, the first equation in (2.4), implies

$$P^T(\hat{A}\hat{\mathbf{x}} + C^T \boldsymbol{\lambda}) = P^T \hat{\mathbf{f}}, \quad \text{or} \quad P^T \hat{A}\hat{\mathbf{x}} = P^T \hat{\mathbf{f}},$$

showing that \mathbf{x} solves (2.3).

The proof of the second part of the theorem is straightforward. \square

Note that the uniqueness of \mathbf{x} is not guaranteed in the settings of Theorem 2.2, even if we assume that P has full column rank and \hat{A} is invertible. Similarly, the uniqueness of $\boldsymbol{\lambda}$ does not follow from the additional assumption that C has full row rank and \hat{A} is invertible.

2.4. A main example of matrices P and C . Below we discuss an application of the main theorem to a slightly more general case of finite element discretization. This is the main example we have in mind in the application to $H(\text{div})$ bilinear form considered in the present paper.

EXAMPLE 2.1. *In a finite element setting, we may think of the following P originating from a generally non-conforming finite element space.*

Assume, that we have elements (or more generally subdomains that are unions of finite elements). We also have interfaces between these substructures (original elements or subdomains). There are degrees of freedom interior, “i”, to the substructures. We also have dofs on the interfaces. In this setting we assume that on the interfaces we have dofs that are master, “m”, and slave, “s”.

Introduce the matrices P and C with the described blocks of i, m, and s-dofs,

$$P = \begin{bmatrix} I_i & 0 \\ 0 & I_m \\ 0 & W_{sm} \end{bmatrix} \quad \text{and} \quad C = \begin{bmatrix} 0 & -W_{sm} & I_s \end{bmatrix}.$$

The 3-by-2 block-form of P above, corresponds to the interior and master dofs (for its columns) and interior, master and slave dofs (for its rows). The block W represents the mapping that determines the slave dofs in terms of the master ones. Finally, the matrix \hat{A} , is the block-diagonal matrix, with blocks assembled for the individual substructures (or simply the element matrices).

As before, we assume that \hat{A} is invertible, which is the case if we have a mass term added to a semidefinite term, like the $H(\text{div})$ bilinear form we consider in this paper.

EXAMPLE 2.2. *Consider the case when the solution space is $H(\text{div})$ -conforming, and introduce a multiplier finite element space, $\mathcal{M} \subset L^2(\mathcal{I})$ on the interface \mathcal{I} between elements (or substructures), see Figure 5.1 for illustration.*

If we denote the broken solution space by $\hat{\mathcal{V}}$, then the matrix C can be derived from the bilinear form:

$$c(\hat{\mathbf{u}}, \lambda) = \int_{\mathcal{I}} [\hat{\mathbf{u}} \cdot \mathbf{n}] \lambda, \quad \hat{\mathbf{u}} \in \hat{\mathcal{V}}, \lambda \in \mathcal{M}.$$

Above, $[\hat{\mathbf{u}} \cdot \mathbf{n}]$ stands for the jump of the normal component of $\hat{\mathbf{u}}$ across the interface \mathcal{I} .

Similarly to Example 2.1, for the same P , the matrix C now has the M_s -weighted form

$$C = \begin{bmatrix} 0 & -M_s W_{sm} & M_s \end{bmatrix},$$

where M_s is a mass matrix between the multiplier space \mathcal{M} and the normal trace space of $\hat{\mathcal{V}}$.

3. Relation to static condensation and hybridized mixed finite elements. In this section we show that the hybridized matrix H , (2.5), is closely related to the matrices obtained with two other classical finite element approaches: that of algebraic *static condensation* and that of traditional hybridization used in the mixed finite element method for second order elliptic equations.

3.1. Static condensation. In the setting of Example 2.1, the matrix \hat{A} can be partitioned into a two-by-two block from with its first block corresponding to the interior dofs (with respect to the substructures). The second block corresponds to the master and slave dofs combined, i.e., we have

$$\hat{A} = \begin{bmatrix} \hat{A}_{ii} & \hat{A}_{ib} \\ \hat{A}_{bi} & \hat{A}_{bb} \end{bmatrix}. \quad (3.1)$$

We notice that \hat{A}_{ii} is block-diagonal, since the interior dofs in one substructure do not couple with interior dofs in any other substructure. The Schur complement

$$\hat{S} = \hat{A}_{bb} - \hat{A}_{bi} \hat{A}_{ii}^{-1} \hat{A}_{ib},$$

is SPD, hence invertible. It acts on vectors corresponding to the interface dofs “ b ” (combined slave and master ones). Now, consider the Schur complement $H = C \hat{A}^{-1} C^T$ from (2.5) for the hybridized system (2.4). Since $C = [0, -W, I]$, and

$$\hat{A}^{-1} = \begin{bmatrix} * & * \\ * & \hat{S}^{-1} \end{bmatrix},$$

we easily see that

$$H = C \hat{A}^{-1} C^T = [-W, I] \hat{S}^{-1} [-W, I]^T,$$

while the *static condensation* matrix, i.e., the reduced matrix for the master dofs is

$$S = \begin{bmatrix} I \\ W \end{bmatrix}^T \hat{S} \begin{bmatrix} I \\ W \end{bmatrix}. \quad (3.2)$$

In the case of finite element matrices, when the coupling across elements (or more generally, across substructures) occurs only via interface dofs (no vertex and edge dofs), one can decouple each interface dof into exactly two copies, and let $W = -I$. Examples of such elements are the Raviart–Thomas ($H(\text{div})$ -conforming elements); and also, the H^1 -non-conforming Crouzeix–Raviart elements.

In this setting \hat{A} is block-diagonal, and also \hat{S} is block-diagonal (substructure-by-substructure). Thus, to form the hybridized Schur complement H , we need to assemble the inverses of the local substructure Schur complements, whereas to form the static condensation matrix S , we need to assemble the local substructure Schur complements.

In other words, we may view the hybridization approach as a sort of a “dual” technique to the static condensation approach. This has important consequences for the construction of solvers for the respective problems. For example, we can expect that solvers for S will have the same nature as solvers for the original matrix A , whereas solvers for H , will need preconditioners that are effective in the dual to the original trace space. This is the case for the $H(\text{div})$ problem, as observed in [25].

3.2. Hybridized mixed finite element method. We next consider traditional hybridization for mixed finite elements, cf. [25], applied in the settings of the $H(\text{div})$ problem: find $\mathbf{u} \in H(\text{div}; \Omega)$ such that

$$a_{\text{div}}(\mathbf{u}, \mathbf{v}) = (\alpha \text{div } \mathbf{u}, \text{div } \mathbf{v}) + (\beta \mathbf{u}, \mathbf{v}) = (\mathbf{g}, \mathbf{v}) \quad \forall \mathbf{v} \in H(\text{div}; \Omega), \quad (3.3)$$

where the coefficients α and β are positive and in general heterogeneous. In this case, \widehat{A} has the following special form

$$\widehat{A} = \widehat{B}^T \widehat{W}^{-1} \widehat{B} + \widehat{M}. \quad (3.4)$$

By introducing an additional unknown $q = \text{div } \mathbf{u}$, a mixed formulation of (3.3) can be written as: find $(\mathbf{u}, q) \in H(\text{div}; \Omega) \times L^2(\Omega)$ such that

$$\begin{aligned} (\beta \mathbf{u}, \mathbf{v}) + (q, \text{div } \mathbf{v}) &= (\mathbf{g}, \mathbf{v}) & \forall \mathbf{v} \in H(\text{div}; \Omega), \\ (\text{div } \mathbf{u}, p) - (\alpha^{-1} q, p) &= 0 & \forall p \in L^2(\Omega). \end{aligned} \quad (3.5)$$

Notice that (3.5) coincides with the mixed formulation of the scalar second order elliptic problem

$$-\text{div}(\beta^{-1} \nabla q) + \alpha^{-1} q = g \quad (3.6)$$

by letting $\mathbf{u} = \beta^{-1} \nabla q$. Hence, (3.5) can be discretized by the hybridized mixed finite element methods designed for (3.6), c.f. [13], resulting in a discrete problem of the form

$$\begin{bmatrix} \widehat{M} & \widehat{B}^T & C^T \\ \widehat{B} & -\widehat{W} & 0 \\ C & 0 & 0 \end{bmatrix} \begin{bmatrix} \widehat{\mathbf{x}} \\ q \\ \boldsymbol{\lambda} \end{bmatrix} = \begin{bmatrix} \widehat{\mathbf{f}} \\ 0 \\ 0 \end{bmatrix}.$$

The corresponding reduced problem for the Lagrange multipliers reads

$$\widetilde{H} \boldsymbol{\lambda} = [C \quad 0] \begin{bmatrix} \widehat{M} & \widehat{B}^T \\ \widehat{B} & -\widehat{W} \end{bmatrix}^{-1} \begin{bmatrix} C^T \\ 0 \end{bmatrix} \boldsymbol{\lambda} = [C \quad 0] \begin{bmatrix} \widehat{M} & \widehat{B}^T \\ \widehat{B} & -\widehat{W} \end{bmatrix}^{-1} \begin{bmatrix} \widehat{\mathbf{f}} \\ 0 \end{bmatrix},$$

which is identical to (2.5) because of (3.4) and the fact that the (1,1) entry in the above inverse is the inverse of the Schur complement $\widehat{M} + \widehat{B}^T \widehat{W}^{-1} \widehat{B}$. In other words, $H = \widetilde{H}$, so the algebraic hybridization approach is identical when applied to the mixed or second order version of the problem.

4. Scalable algebraic $H(\text{div})$ preconditioning. In this section we propose several scalable algebraic multigrid approaches for finite element discretizations of the $H(\text{div})$ form $a_{\text{div}}(\cdot, \cdot)$ based on the methods discussed in the previous sections. Due to their scalability on challenging practical problems, we base our preconditioners on the parallel algebraic multigrid approaches available in the *hypre* library, [4]. Specifically we take advantage of the BoomerAMG [19], AMS [23] and ADS [24] methods in *hypre*, targeting H^1 , $H(\text{curl})$ and $H(\text{div})$ discretizations respectively.

We first consider the static condensation Schur complement S , (3.2), and discuss approaches for its preconditioning. Since S acts in general on traces of functions from a given space ($H(\text{div})$, $H(\text{curl})$, or H^1), a suitable preconditioner for S will be some approximation to the Schur complement of an (optimal) preconditioner for the original matrix A . Of course, for efficiency, we would like to build a preconditioner

directly for the (sparse) matrix S and not for the original matrix A . Such preconditioners are discussed in [10] where it is shown, both theoretically and practically, that BoomerAMG and AMS work well on Schur complements of H^1 and $H(\text{curl})$ discretizations respectively. Similar analysis for the $H(\text{div})$ case was recently performed in [5]. In all three cases, the summary of the stable decomposition theory is that if BoomerAMG/AMS/ADS works for a particular problem, it will also work, purely algebraically, for a Schur complement of the problem. Thus, the $H(\text{div})$ Schur complement S considered in this paper can be efficiently preconditioned simply with a direct application of ADS.

We next consider preconditioning approaches for the hybridized matrix H . Based on the connection with mixed methods from the previous section we argue that one suitable preconditioner for the hybridized Schur complement H in the case of the $H(\text{div})$ problem is an H^1 -based AMG built from the matrix H . The rest of this section is devoted by providing arguments for this choice, by exploring the “near-nullspace” of H , i.e. the set of its low-frequency eigenmodes, that is critical in AMG theory.

Let us consider a norm $\|\cdot\|$ for the space of Lagrange multiplier,

$$\|\boldsymbol{\lambda}\|^2 = \sum_{\tau \in \mathcal{T}_h} \left(h_\tau \|\boldsymbol{\lambda}\|_{\partial\tau}^2 + \frac{1}{h_\tau} \|\boldsymbol{\lambda} - m_\tau(\boldsymbol{\lambda})\|_{\partial\tau}^2 \right),$$

where \mathcal{T}_h is a finite element mesh and $m_\tau(\boldsymbol{\lambda}) = \frac{1}{|\partial\tau|} \int_{\partial\tau} \boldsymbol{\lambda} \, ds$. It is proven in [14] that \tilde{H} is spectrally equivalent to $\|\cdot\|$, so we can deduce that H has a small near-nullspace containing only the constant functions, as opposed to the large near-nullspace of the original system A . Therefore, the hybridized Schur complement H is “ H^1 -like”, which motivates the use of H^1 -based AMG for preconditioning.

In fact, by exploiting \tilde{H} , one can see that H has the explicit form:

$$H = \tilde{H} = C(\widehat{M}^{-1} - \widehat{M}^{-1}\widehat{B}^T(\widehat{W} + \widehat{B}\widehat{M}^{-1}\widehat{B}^T)^{-1}\widehat{B}\widehat{M}^{-1})C^T.$$

In the above expression, \widehat{W} is an L^2 mass matrix while $\widehat{B}\widehat{M}^{-1}\widehat{B}^T$ resembles a weighted discrete Laplacian. Hence, $\widehat{B}\widehat{M}^{-1}\widehat{B}^T \gg \widehat{W}$ and so the near-nullspace of H is characterized by the nullspace of the matrix $C\widehat{Y}C^T$, where

$$\widehat{Y} = \widehat{M}^{-1} - \widehat{M}^{-1}\widehat{B}^T(\widehat{B}\widehat{M}^{-1}\widehat{B}^T)^{-1}\widehat{B}\widehat{M}^{-1}.$$

Note that for any $\widehat{\mathbf{x}} \in \text{Range}(\widehat{B}^T)$, there exists $\widehat{\mathbf{y}}$ such that $\widehat{\mathbf{x}} = \widehat{B}^T\widehat{\mathbf{y}}$, so

$$\widehat{Y}\widehat{\mathbf{x}} = \widehat{M}^{-1}\widehat{\mathbf{x}} - \widehat{M}^{-1}\widehat{B}^T(\widehat{B}\widehat{M}^{-1}\widehat{B}^T)^{-1}\widehat{B}\widehat{M}^{-1}\widehat{B}^T\widehat{\mathbf{y}} = \widehat{M}^{-1}\widehat{\mathbf{x}} - \widehat{M}^{-1}\widehat{B}^T\widehat{\mathbf{y}} = 0.$$

Thus, we have

$$\text{Range}(\widehat{B}^T) \subseteq \text{Null}(\widehat{Y}). \quad (4.1)$$

On the other hand, let $\widehat{\mathbf{x}} \in \text{Null}(\widehat{Y})$. Then

$$\widehat{M}^{-1}\widehat{\mathbf{x}} - \widehat{M}^{-1}\widehat{B}^T(\widehat{B}\widehat{M}^{-1}\widehat{B}^T)^{-1}\widehat{B}\widehat{M}^{-1}\widehat{\mathbf{x}} = 0.$$

Consequently, $\widehat{\mathbf{x}} = \widehat{B}^T(\widehat{B}\widehat{M}^{-1}\widehat{B}^T)^{-1}\widehat{B}\widehat{M}^{-1}\widehat{\mathbf{x}}$. So for any $\widehat{\mathbf{y}} \in \text{Null}(\widehat{B})$, we have

$$\begin{aligned} \langle \widehat{\mathbf{x}}, \widehat{\mathbf{y}} \rangle &= \left\langle \widehat{B}^T(\widehat{B}\widehat{M}^{-1}\widehat{B}^T)^{-1}\widehat{B}\widehat{M}^{-1}\widehat{\mathbf{x}}, \widehat{\mathbf{y}} \right\rangle \\ &= \left\langle (\widehat{B}\widehat{M}^{-1}\widehat{B}^T)^{-1}\widehat{B}\widehat{M}^{-1}\widehat{\mathbf{x}}, \widehat{B}\widehat{\mathbf{y}} \right\rangle = 0 \end{aligned}$$

Hence,

$$\text{Null}(\widehat{Y}) \subseteq \text{Null}(\widehat{B})^\perp = \text{Range}(\widehat{B}^T).$$

The above inclusion relation and (4.1) imply that

$$\text{Null}(\widehat{Y}) = \text{Range}(\widehat{B}^T).$$

Therefore, in order to know what $\text{Null}(C\widehat{Y}C^T)$ is, we should find out

$$\text{Range}(C^T) \cap \text{Range}(\widehat{B}^T).$$

Note that the constraint matrix C enforces the continuity of the master and slave dofs on the interface (cf. Example 2.1), so $\text{Range}(C^T)$ is orthogonal to the subspace spanned by all the interior dofs. In other words, $\widehat{\mathbf{x}}$ is in $\text{Range}(C^T)$ only if every entry corresponding to an interior dof is zero. So we are looking for the vectors in $\text{Range}(\widehat{B}^T)$ such that entries corresponding to interior dofs are zero. Recall that \widehat{B} comes from the bilinear form $(\text{div } \mathbf{u}, p)$. In the case of Raviart-Thomas elements, constants are the only p such that $(\text{div } \mathbf{u}, p) = 0$ for all the \mathbf{u} associated with interior dofs (bubbles). Hence, we deduce that

$$\text{Null}(C\widehat{Y}C^T) = \left\{ \boldsymbol{\lambda} \mid C^T \boldsymbol{\lambda} \in \text{span}\{\widehat{B}^T \mathbf{1}\} \right\},$$

where $\mathbf{1}$ is the coefficient vector of the constant 1 function in the corresponding discrete space. This clearly shows that $\dim(\text{Null}(C\widehat{Y}C^T)) \leq 1$.

5. Implementation details. In this section we provide some details for the practical application of the presented approaches as implemented in the finite element library MFEM [2].

The implementation is contained in class `Hybridization` which can be used either directly, or more conveniently through the `BilinearForm` class. The prolongation operator P is not directly constructed, instead, its action can be performed using the methods in class `FiniteElementSpace`. The constraints matrix C is constructed as illustrated in Example 2.2, based on a specified multiplier finite element space and a given bilinear form.

During a construction stage, the element matrices are reordered and stored in the 2×2 block form (3.1), see Figure 5.1 for illustration. Recall that the i - and b -block unknowns correspond to the element interior and boundary (or interface) degrees of freedom. Any rows and columns associated with essential degrees of freedom (e-dofs) are eliminated. Algebraically, the interior dofs can be defined as those corresponding to zero columns in the C matrix. In other words, C has the 1×2 block form

$$C = \begin{bmatrix} 0 & C_b \end{bmatrix}.$$

As a consequence, the matrix H of the hybridized system (2.5) can be computed as

$$H = C\widehat{A}^{-1}C^T = C_b\widehat{S}_b^{-1}C_b^T,$$

where $\widehat{S}_b = \widehat{A}_{bb} - \widehat{A}_{bi}\widehat{A}_{ii}^{-1}\widehat{A}_{ib}$ is the Schur complement of \widehat{A} which can be formed independently for each element in the mesh. In MFEM, this is performed using element-wise block LU factorizations of the form

$$\begin{bmatrix} \widehat{A}_{ii} & \widehat{A}_{ib} \\ \widehat{A}_{bi} & \widehat{A}_{bb} \end{bmatrix} = \begin{bmatrix} \widehat{L}_i & 0 \\ \widehat{L}_{bi} & \widehat{I}_b \end{bmatrix} \begin{bmatrix} \widehat{U}_i & \widehat{U}_{ib} \\ 0 & \widehat{S}_b \end{bmatrix}$$

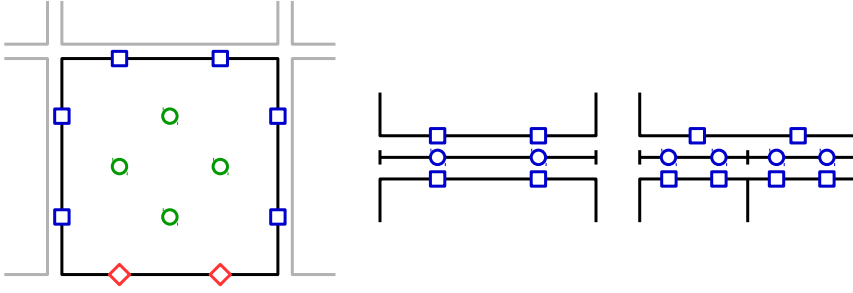


FIG. 5.1. Left: local RT_1 dofs: i -dofs (green circles), b -dofs (blue squares), and e -dofs (red diamonds). Center/Right: dofs associated with a conforming (center) and a non-conforming (right) mesh face: RT_1 dofs to match (blue squares) and multiplier dofs (blue circles).

to compute the Schur complements \widehat{S}_b which are then themselves LU-factorized, allowing simple multiplication of any vector or matrix with \widehat{S}_b^{-1} .

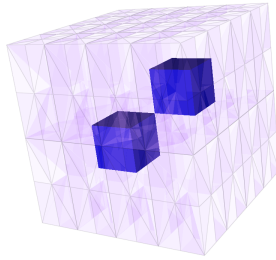
Note that for Robin-type boundary conditions, one needs to assemble contributions to the global system matrix A coming from integration over boundary faces. In MFEM, such face matrices are assembled into the element matrix of the element adjacent to the corresponding face. The rest of the hybridization procedure remains the same.

6. Numerical tests. To validate the parallel scalability of the proposed solvers, in this section we present several weak scaling tests, where the number of degrees of freedom per processor is held to be about the same while the number of processors is increased. All the experiments except the ones in Section 6.3 are performed on the cluster Sierra at Lawrence Livermore National Laboratory (LLNL). Sierra has a total of 1944 nodes (Intel Xeon EP X5660 @ 2.80 GHz), each of which has 12 cores and 24 GB of memory. The numerical results are generated using the libraries MFEM [2] and *hypre* [1] developed at LLNL.

6.1. Soft hard materials. Consider solving (3.3) on the unit cube, i.e. $\Omega = [0, 1]^3$, with the source function \mathbf{g} being $[1, 1, 1]^T$. Let $\Omega_i = [\frac{1}{4}, \frac{1}{2}]^3 \cup [\frac{1}{2}, \frac{3}{4}]^3$. We consider $\alpha \equiv 1$ in Ω , whereas

$$\beta = \begin{cases} 1 & \text{in } \Omega \setminus \Omega_i \\ 10^p & \text{in } \Omega_i \end{cases}, \quad p \in \{-8, -4, 0, 4, 8\}.$$

This example is intended to test the robustness of the solvers against coefficient jumps.



We discretize (3.3) by Raviart-Thomas elements (RT_k) on hexahedral meshes. In

order to better contrast the effect of higher order discretizations, the initial meshes in the weak scaling tests are chosen so that the problem size is the same for discretizations of different orders, see Table 6.1. The PCG stopping criterion is a reduction in the l_2

TABLE 6.1
Initial mesh sizes in the weak scaling tests in Section 6.1

Finite element	RT_0	RT_1	RT_3
Initial mesh	$64 \times 64 \times 32$	$32 \times 32 \times 16$	$16 \times 16 \times 8$

residual by a factor of 10^{-12} . The time to solution and number of PCG iterations (in parentheses) for the proposed approaches, as well as ADS, are reported in Tables 6.2–6.4. Here, the time to solution for the hybridization approach includes the formation time of the hybridization Schur complement H , the setup time of AMG (BoomerAMG [19]), PCG solving time, and the time for recovering the original solution by back substitution. Similarly, the time to solution for the static condensation approach includes the formation time of S (cf. Section 3), ADS setup time, PCG solving time, and back substitution. Lastly, the time to solution for “ADS” is simply ADS setup time and PCG solving time. Our results show that all the solvers have good weak

TABLE 6.2
Time to solution of different solvers: RT_0 on hexahedral meshes

#proc	Size	$p = -8$	$p = -4$	$p = 0$	$p = 4$	$p = 8$
Hybridization + AMG						
3	401,408	3.39 (24)	3.5 (26)	3.55 (27)	3.56 (27)	3.44 (26)
24	3,178,496	7.29 (29)	7.43 (31)	7.34 (30)	7.29 (30)	7.35 (30)
192	25,296,896	8.28 (33)	8.54 (37)	8.45 (32)	8.3 (32)	8.3 (33)
1,536	201,850,880	9.79 (37)	10.33 (39)	9.98 (36)	10.28 (38)	10.17 (36)
ADS						
3	401,408	17.35 (16)	17.51 (16)	15.94 (13)	20.54 (19)	20.11 (21)
24	3,178,496	36.94 (18)	36.91 (18)	35.69 (16)	38.76 (21)	40 (23)
192	25,296,896	42.54 (20)	42.39 (20)	40.99 (17)	43.75 (22)	45.7 (25)
1,536	201,850,880	49.91 (21)	49.64 (21)	47.73 (19)	52.93 (25)	52.62 (27)

scaling and robustness with respect to coefficient jumps. In all the cases, while both the hybridization and static condensation solvers give shorter solving time than ADS, the hybridization approach is the fastest. Moreover, as the finite element order goes higher, discrepancy in the solution time between the solvers becomes more significant even though the problem size is the same. In particular, for the RT_3 discretization, hybridization is in general 4 times faster than static condensation, and 20 times faster than ADS.

6.2. The crooked pipe problem. This example deals with large coefficient jumps and highly stretched elements, see Figure 6.2. The coefficients α and β are both piecewise-constant functions such that

$$(\alpha, \beta) = \begin{cases} (1.641, 0.2) & \text{in red region,} \\ (0.00188, 2000) & \text{in blue region.} \end{cases}$$

The setup of the experiments is the same as in Section 6.1, and the weak scaling results are reported in Table 6.5. Note that we were running out of memory when setting up ADS for RT_3 (indicated by “*”), which shows that the hybridization and static

TABLE 6.3
Time to solution of different solvers: RT_1 on hexahedral meshes

#proc	Size	$p = -8$	$p = -4$	$p = 0$	$p = 4$	$p = 8$
Hybridization + AMG						
3	401,408	3.35 (27)	3.39 (28)	3.46 (28)	3.43 (29)	3.46 (28)
24	3,178,496	5.97 (30)	6.14 (33)	6.06 (32)	5.95 (31)	6.11 (32)
192	25,296,896	6.85 (36)	7.03 (37)	7.25 (36)	7 (35)	7.43 (35)
1,536	201,850,880	7.84 (39)	9.17 (41)	8.17 (39)	8.83 (41)	9.85 (40)
Static condensation + ADS						
3	401,408	19.69 (15)	19.65 (15)	18.23 (12)	20.92 (17)	21.91 (18)
24	3,178,496	40.5 (19)	40.69 (19)	36.77 (15)	42.42 (21)	43.51 (22)
192	25,296,896	46.48 (21)	46.81 (21)	42.63 (17)	48.68 (23)	51.62 (26)
1,536	201,850,880	54.78 (23)	54.43 (22)	50.38 (19)	59.4 (26)	61.56 (29)
ADS						
3	401,408	34.73 (18)	34.53 (17)	30.66 (14)	38.93 (22)	41.44 (24)
24	3,178,496	60.9 (20)	61.13 (20)	55.19 (16)	68.06 (25)	71.44 (27)
192	25,296,896	68.55 (22)	67.39 (21)	62.5 (18)	77.74 (28)	81.1 (30)
1,536	201,850,880	78.8 (24)	80.99 (24)	72.89 (20)	90.74 (31)	102.93 (37)

TABLE 6.4
Time to solution of different solvers: RT_3 on hexahedral meshes

#proc	Size	$p = -8$	$p = -4$	$p = 0$	$p = 4$	$p = 8$
Hybridization + AMG						
3	401,408	9.27 (33)	9.46 (35)	9.42 (37)	9.62 (38)	9.51 (38)
24	3,178,496	13.1 (41)	12.91 (43)	14 (44)	13.53 (44)	13.25 (44)
192	25,296,896	14.81 (48)	15.58 (50)	15.26 (50)	14.71 (50)	16.4 (50)
1,536	201,850,880	16.8 (53)	16.33 (56)	16.63 (56)	17.67 (56)	19.06 (56)
Static condensation + ADS						
3	401,408	31.38 (12)	31.38 (12)	29.28 (10)	32.65 (13)	32.38 (13)
24	3,178,496	56.09 (15)	55.87 (15)	54.64 (14)	59.06 (17)	59.03 (17)
192	25,296,896	67.01 (18)	67.28 (18)	65.22 (17)	70.43 (20)	70.53 (20)
1,536	201,850,880	83.81 (20)	82.14 (20)	81.69 (19)	85.65 (22)	86.65 (23)
ADS						
3	401,408	184.67 (18)	186.1 (18)	169.27 (14)	188.58 (19)	189.52 (20)
24	3,178,496	253.3 (19)	259.11 (20)	240.87 (16)	269.12 (22)	284.04 (25)
192	25,296,896	288.32 (22)	289.14 (22)	261.95 (17)	305.86 (25)	325.93 (29)
1,536	201,850,880	329.76 (24)	330.46 (23)	301.61 (19)	353.63 (28)	366.94 (31)

condensation approaches are more memory-friendly for high order discretizations. The results in Table 6.5 again suggest that hybridization with AMG is the most efficient solver among the three for this particular problem; it is also observed that the iteration count in the hybridization approach is more steady than the other two.

6.3. Application to radiation diffusion. In this section we compare the proposed approaches when they are used for solving the radiation diffusion equations in flux form, see [9]. This model is often used in astrophysical and inertial confinement fusion (ICF) simulations. We consider a problem with two materials ($k = 1, 2$ below), indicated by blue and red colors in Figure 6.3, and there are no mixed zones. The

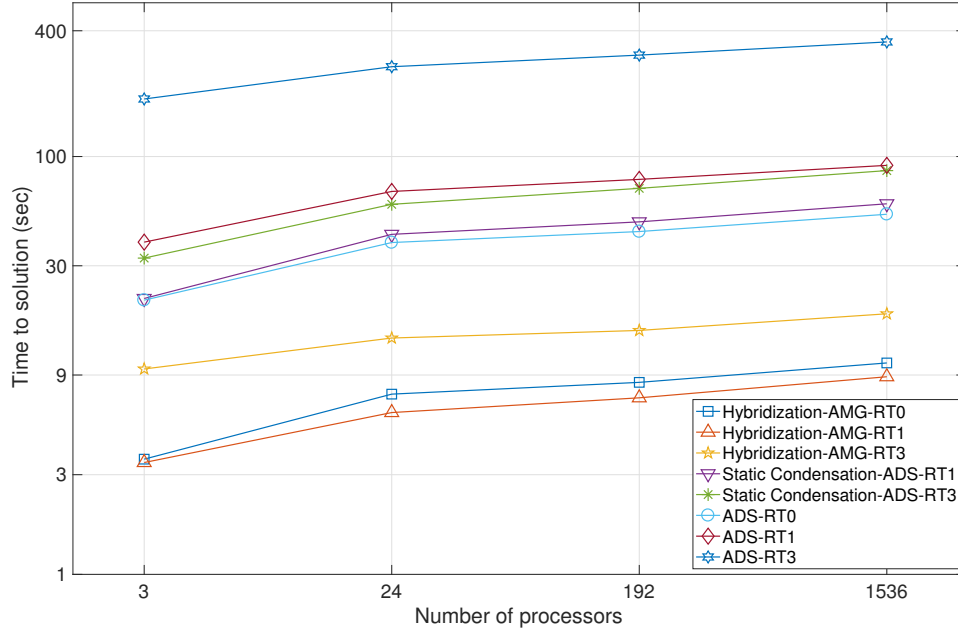
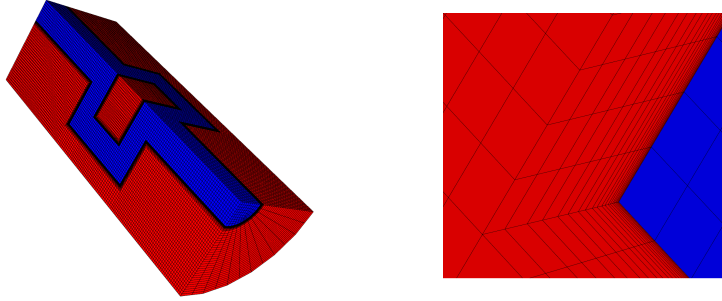
FIG. 6.1. Weak scaling plots in log-log scale for the soft hard materials example when $p = 4$ 

FIG. 6.2. Geometry and material interface of the crooked pipe example

governing equations are

$$\begin{aligned}
 \rho_k \frac{de_k}{dt} &= c\sigma_k(E - B(T(e_k))), \\
 \frac{dE}{dt} + \nabla \cdot F &= -c \sum_k \sigma_k(E - B(T(e_k))), \\
 \frac{1}{3} \nabla E &= - \sum_k \frac{\sigma_k}{c} F,
 \end{aligned} \tag{6.1}$$

subject to the boundary conditions specified in Figure 6.3. Here e_k, ρ_k, σ_k are the internal energy, density and opacity, respectively, of material k , E is radiation energy, F is radiation flux, B is the Planck's function for black-body radiation, and c is the

TABLE 6.5
Solution time for the crooked pipe example

#proc	Size	RT_0	RT_1	RT_3
Hybridization + AMG				
12	2,805,520	8.56 (34)	8.44 (33)	22.41 (42)
96	22,258,240	13.4 (37)	12.45 (36)	29.97 (44)
768	177,322,240	17.82 (45)	15.28 (45)	37.13 (49)
6,144	1,415,603,200	23.73 (54)	21.36 (55)	43.01 (60)
Static condensation + ADS				
12	2,805,520	73.76 (52)	98.73 (43)	190.53 (40)
96	22,258,240	126.87 (80)	177.71 (74)	305.51 (67)
768	177,322,240	191.67 (117)	291.03 (122)	481.28 (107)
6,144	1,415,603,200	274.09 (168)	463.95 (190)	715.79 (158)
ADS				
12	2,805,520	73.76 (52)	174.55 (59)	* (*)
96	22,258,240	126.87 (80)	291.4 (93)	* (*)
768	177,322,240	191.67 (117)	442 (139)	* (*)
6,144	1,415,603,200	274.09 (168)	706.5 (212)	* (*)

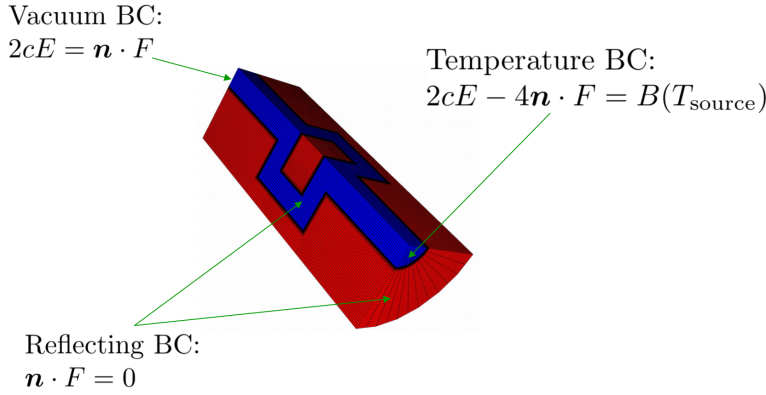


FIG. 6.3. Boundary conditions for the radiation diffusion problem

speed of light. The temperature boundary condition heats up one of the ends of the pipe, causing an increase of the radiation field E and its diffusion throughout the domain.

The discrete approximations of E and e_k are in the finite elements space $Q_r \subset L^2$, consisting of piecewise polynomials of degree r , while the flux F is approximated in the Raviart-Thomas space RT_r . For stability reasons the time stepping of e_k and E is implicit, which results in a nonlinear problem in each time step, as $B(T(e_k))$ is nonlinear. Newton's method is used to solve the resulting system. As E and e_k are discontinuous, they can be eliminated locally during each Newton iteration, which is inexpensive and inherently parallel. Upon eliminating E and e_k , an $H(\text{div})$ linear system for F is obtained, which we use to test the performance of the two proposed approaches, as well as AMS (2D) and ADS (3D).

Because each method ultimately solves a different linear system, this example is used to obtain better perception of the execution time needed for each method to obtain similar solution accuracy with respect to the original system. Starting

with identical initial conditions, each computation performs exactly one linear solve, and then the F residual is calculated from the definition of the nonlinear system. Execution times are presented for computations reaching similar residuals. For this particular example, this is achieved by setting the relative tolerances to $1e-6$, $1e-5$ and $1e-12$ for AMS/ADS, static condensation+AMS/ADS, and hybridization+AMG, respectively.

As observed in Tables 6.6 and 6.7, even though the hybridized system must be solved to a much lower relative tolerance, the hybridization approach still has the shortest solving time, followed by the static condensation and then ADS. Except for RT_0 in the 2D case, the hybridization approach is at least 10 times faster than AMS/ADS, which is a substantial improvement.

TABLE 6.6
2D problem with $\#dof=324712$.

Method	RT_0		RT_1			RT_3		
	HB	AMS	HB	SC	AMS	HB	SC	AMS
Time	3.05	15.35	1.11	7.29	18.63	1.35	6.21	35.68
GMRES iterations	100	245	50	129	200	73	130	190
Final residual $\times 1e-5$	2.09	5.34	9.65	3.76	6.64	3.61	3.58	2.01

TABLE 6.7
3D problem with $\#dof=124208$.

Method	RT_0		RT_1			RT_3		
	HB	ADS	HB	SC	ADS	HB	SC	ADS
Time	0.39	3.86	0.58	4.39	10.06	3.02	12.44	67.68
GMRES iterations	24	42	27	23	43	28	18	46
Final residual $\times 1e-5$	8.23	3.87	1.48	7.00	2.54	1.01	0.882	1.19

6.4. The SPE10 benchmark. Our last numerical example is the SPE10 benchmark coefficient [12] from the reservoir simulation community. This coefficient is well-known for its multi-scale heterogeneity and anisotropy. The initial mesh is a $60 \times 220 \times 85$ hexahedral grid, with the size of each cell being $20 \times 10 \times 2$. β is taken to be the SPE10 coefficient (see Figure 6.4), and $\alpha \equiv 1$. The time spent on different components of the solution process for the hybridization approach and ADS are shown in Tables 6.8 and 6.9 respectively. This example also demonstrates the superiority in terms of performance of the hybridization solver.

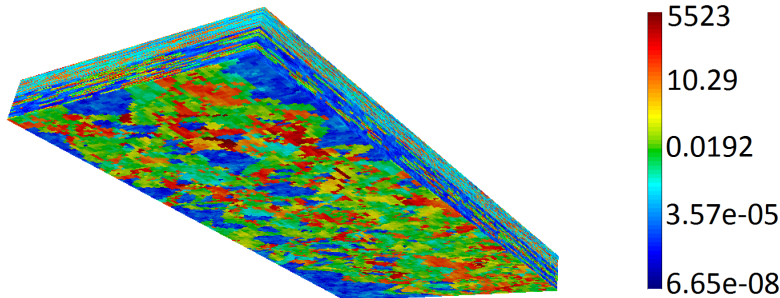


FIG. 6.4. The SPE10 coefficient

TABLE 6.8
The SPE10 example solved by hybridization and AMG

#proc	Size	Hybridize	AMG setup	PCG Solve	Back sub.	Total time
3	3,403,000	21.3	2.21	18.6	0.51	42.62 (48)
24	27,076,000	68.75	3.76	23.59	0.62	96.72 (45)
192	216,016,000	111.82	6.93	27.85	0.63	147.22 (44)
1,536	1,725,760,000	131.85	9.6	29.58	0.65	171.68 (40)

TABLE 6.9
The SPE10 example solved by ADS

#proc	Size	ADS setup	PCG solve	Total time
3	3,403,000	85.77	405.76	491.53 (123)
24	27,076,000	290.17	1416.49	1706.66 (300)
192	216,016,000	492.11	3529.19	4021.3 (635)
1,536	1,725,760,000	585.7	5977.23	6562.93 (959)

7. Conclusion. In this paper, two popular techniques in finite elements, hybridization and static condensation, were studied and compared. Both of these two techniques lead to a reduced system of the same size. The formation of the reduced system involves inversion of independent local matrices, which can be done in parallel. We also discuss suitable preconditioning strategies using various algebraic multigrid methods for the respective reduced systems. In particular, we demonstrate that if BoomerAMG/AMS/ADS work well for the original problem, then they also work well for the reduced systems obtained from static condensation. On the other hand, AMG for H^1 -equivalent problems is actually a well-suited preconditioner for the reduced system resulting from hybridization of $H(\text{div})$ problems. We presented several numerical examples comparing the performance of the proposed approaches, as well as solving the original problem directly by ADS/AMS. Our results show good weak scaling of all of the proposed approaches. In general, for $H(\text{div})$ problems, the approach using hybridization and AMG is more efficient than the approach using static condensation and ADS/AMS, while both of these approaches are faster than a direct application of ADS/AMS to the original problem. In fact, we observed substantial savings in the solve time if the hybridization approach is used, especially for higher order discretizations. Implementation of the two approaches are freely available in MFEM [2].

REFERENCES

- [1] *hypre: A library of high performance preconditioners*. <http://www.llnl.gov/CASC/hypre/>. 1, 11
- [2] *MFEM: Modular finite element methods*. mfem.org. 1, 10, 11, 17
- [3] D. N. ARNOLD AND F. BREZZI, *Mixed and nonconforming finite element methods : implementation, postprocessing and error estimates*, ESAIM: Mathematical Modelling and Numerical Analysis - Modlisation Mathematique et Analyse Numrique, 19 (1985), pp. 7–32. 1
- [4] A. BAKER, R. FALGOUT, T. KOLEV, AND U. YANG, *Scaling hypre's multigrid solvers to 100,000 cores*, in High Performance Scientific Computing: Algorithms and Applications, Springer, 2012, pp. 261–279. LLNL-JRNL-479591. 8
- [5] A. BARKER, V. DOBREV, J. GOPALAKRISHNAN, AND V. KOLEV, *A scalable preconditioner for a DPG method*, (submitted). 2, 9
- [6] D. BOFFI, F. BREZZI, AND M. FORTIN, *Mixed Finite Element Methods and Applications*, Springer Series in Computational Mathematics 44, Springer Berlin Heidelberg, 2013. 1
- [7] F. BREZZI AND M. FORTIN, *Mixed and Hybrid Finite Element Methods*, Springer-Verlag New

- York, Inc., New York, NY, USA, 1991. [4](#)
- [8] F. BREZZI AND D. MARINI, *A survey on mixed finite element approximations*, IEEE Transactions on Magnetics, 30 (1994), pp. 3547–3551. [2](#)
 - [9] T. BRUNNER, *Forms of approximate radiation transport*, Sandia National Laboratory Technical Report, SAND2002-1778 (2002). [1](#), [13](#)
 - [10] T. A. BRUNNER AND T. V. KOLEV, *Algebraic multigrid for linear systems obtained by explicit element reduction*, SIAM J. Sci. Comput., 33 (2011), pp. 2706–2731. [2](#), [9](#)
 - [11] Z. CAI, R. LAZAROV, T. A. MANTEUFFEL, AND S. F. MCCORMICK, *First-order system least squares for second-order partial differential equations: Part I*, SIAM Journal on Numerical Analysis, 31 (1994), pp. 1785–1799. [1](#)
 - [12] M. A. CHRISTIE AND M. J. BLUNT, *Tenth SPE comparative solution project: A comparison of upscaling techniques*, Society of Petroleum Engineers, (2001). [16](#)
 - [13] B. COCKBURN AND J. GOPALAKRISHNAN, *A characterization of hybridized mixed methods for second order elliptic problems*, SIAM Journal on Numerical Analysis, 42 (2004), pp. 283–301. [8](#)
 - [14] ———, *Error analysis of variable degree mixed methods for elliptic problems via hybridization*, Mathematics of Computation, 74 (2005), p. 16531677. [2](#), [9](#)
 - [15] ———, *New hybridization techniques*, GAMM-Mitteilungen, 28 (2005), pp. 154–182. [2](#)
 - [16] C. R. DOHRMANN, *A preconditioner for substructuring based on constrained energy minimization*, SIAM Journal on Scientific Computing, 25 (2003), pp. 246–258. [2](#)
 - [17] B. X. FRAELJIS DE VEUBEKE, *Displacement and equilibrium models in the finite element method*, in Stress Analysis, O. C. Zienkiewicz and G. S. Holister, eds., John Wiley & Sons, New York, 1965, pp. 145–197. [1](#)
 - [18] R. J. GUYAN, *Reduction of stiffness and mass matrices*, AIAA Journal, 3 (1965), p. 380. [2](#)
 - [19] V. E. HENSON AND U. M. YANG, *BoomerAMG: A parallel algebraic multigrid solver and preconditioner*, Applied Numerical Mathematics, 41 (2002), pp. 155 – 177. [8](#), [12](#)
 - [20] R. HIPTMAIR AND J. XU, *Nodal auxiliary space preconditioning in $H(\text{curl})$ and $H(\text{div})$ spaces*, SIAM Journal on Numerical Analysis, 45 (2007), pp. 2483–2509. [1](#)
 - [21] B. M. IRONS, *Structural eigenvalue problems – elimination of unwanted variables*, AIAA Journal, 3 (1965), pp. 961–962. [2](#)
 - [22] E. KIKINZON, Y. KUZNETSOV, K. LIPNIKOV, AND M. J. SHASHKOV, *Approximate static condensation algorithm for solving multi-material diffusion problems on mesh non-aligned with material interfaces*, LANL Technical Report, LA-UR-17-22479 (2017). [5](#)
 - [23] T. V. KOLEV AND P. S. VASSILEVSKI, *Parallel auxiliary space AMG solver for $H(\text{curl})$ problems*, J. Comput. Math., 27 (2009), pp. 604–623. [1](#), [8](#)
 - [24] T. V. KOLEV AND P. S. VASSILEVSKI, *Parallel auxiliary space AMG solver for $H(\text{div})$ problems*, SIAM Journal on Scientific Computing, 34 (2012), pp. A3079–A3098. [1](#), [8](#)
 - [25] C. S. LEE AND P. S. VASSILEVSKI, *Parallel solver for $H(\text{div})$ problems using hybridization and AMG*, Springer International Publishing, Cham, 2017, pp. 69–80. [2](#), [7](#), [8](#)
 - [26] D.-S. OH, O. B. WIDLUND, S. ZAMPINI, AND C. R. DOHRMANN, *BDDC algorithms with deluxe scaling and adaptive selection of primal constraints for Raviart-Thomas vector fields*, Mathematics of Computation, (to appear). [2](#)
 - [27] P. S. VASSILEVSKI AND U. VILLA, *A block-diagonal algebraic multigrid preconditioner for the Brinkman problem*, SIAM Journal on Scientific Computing, 35 (2013), pp. S3–S17. [1](#)
 - [28] E. L. WILSON, *Structural analysis of axisymmetric solids*, AIAA Journal, 3 (1965), pp. 2269–2274. [2](#)
 - [29] S. ZAMPINI, *PCBDDC: A class of robust dual-primal methods in PETSc*, SIAM Journal on Scientific Computing, 38 (2016), pp. S282–S306. [2](#)
 - [30] S. ZAMPINI AND D. E. KEYES, *On the robustness and prospects of adaptive bddc methods for finite element discretizations of elliptic pdes with high-contrast coefficients*, in Proceedings of the Platform for Advanced Scientific Computing Conference, PASC ’16, New York, NY, USA, 2016, ACM, pp. 6:1–6:13. [2](#)